Current Genetics
https://doi.org/10.1007/s00294-018-0838-4

ORIGINAL ARTICLE

Phosphorylation by Prp4 kinase releases the self-inhibition of FgPrp31 in *Fusarium graminearum*

Xuli Gao[1] · Ju Zhang[1] · Chaoni Song[1] · Kangyi Yuan[1] · Jianhua Wang[2] · Qiaojun Jin[1] · Jin-Rong Xu[1,2]

Received: 15 March 2018 / Revised: 4 April 2018 / Accepted: 11 April 2018

Abstract

Prp31 is one of the key tri-snRNP components essential for pre-mRNA splicing although its exact molecular function is not well studied. In a previous study, suppressor mutations were identified in the *PRP31* ortholog in two spontaneous suppressors of *Fgprp4* mutant deleted of the only kinase of the spliceosome in *Fusarium graminearum*. To further characterize the function of FgPrp31 and its relationship with FgPrp4 kinase, in this study we identified additional suppressor mutations in FgPrp31 and determined the suppressive effects of selected mutations. In total, 28 of the 35 suppressors had missense or nonsense mutations in the C terminus 465–594 aa (CT130) region of FgPrp31. The other 7 had missense or deletion mutations in the 7–64 aa region. The nonsense mutation at R464 in *FgPRP31* resulted in the truncation of CT130 that contains all the putative Prp4 kinase-phosphorylation sites reported in humans, and partially rescued intron splicing defects of *Fgprp4*. The CT130 of FgPrp31 displayed self-inhibitory interaction with the N-terminal 1-463 (N463) region, which was reduced or abolished by the L532P, D534G, or G529D mutation in yeast two-hybrid assays. The N463 region, but not full-length FgPrp31, interacted with the N-terminal region of FgBrr2, one main U5 snRNP protein. The L532P mutation in FgPrp31 increased its interaction with FgBrr2. In contrast, suppressor mutations in FgPrp31 reduced its interaction with FgPrp6, another key component of tri-snRNP. Furthermore, we showed that FgPrp31 was phosphorylated by FgPrp4 in vivo. Site-directed mutagenesis analysis showed that phosphorylation at multiple sites in FgPrp31 is necessary to suppress *Fgprp4*, and S520 and S521 are important FgPrp4-phosphorylation sites. Overall, these results indicated that phosphorylation by FgPrp4 at multiple sites may release the self-inhibitory binding of FgPrp31 and affect its interaction with other components of tri-snRNP during spliceosome activation.

Keywords Prp31 · RNA splicing · Spliceosome · Tri-snRNP · Fungal development

Introduction

Splicing of introns in precursor messenger RNA (pre-mRNA) is achieved by two sequential trans-esterification reactions that are catalyzed by the spliceosome, a dynamic ribonucleoprotein (RNP) complex consisting of U1, U2, U4, U5, and U6 RNA and many structural proteins and splicing factors (Will and Luhrmann 2011). The spliceosome assembly begins with the recognition of the 5′-splicing site (5′ss) and branch point (bp) of introns by U1 and U2 snRNP, respectively, to form complex A. The pre-formed U4/U6–U5 tri-snRNP is then integrated into A-complex to form B-complex, which then undergoes dramatically structural and compositional remodeling during activation, including the unwinding of base-paired U4/U6 and release of U1 and U4. The activated B^* complex catalyzes the first trans-esterification reaction that involves the cleavage at the

Communicated by M. Kupiec.

Electronic supplementary material The online version of this article (https://doi.org/10.1007/s00294-018-0838-4) contains supplementary material, which is available to authorized users.

✉ Qiaojun Jin
jqiaojun@nwafu.edu.cn

✉ Jin-Rong Xu
jinrong@purdue.edu

[1] NWAFU-Purdue Joint Research Center, State Key Laboratory of Crop Stress Biology for Arid Areas, College of Plant Protection, Northwest A&F University, Yangling, Shaanxi, China

[2] Department of Botany and Plant Pathology, Purdue University, West Lafayette, IN, USA

Published online: 18 April 2018

5'ss and formation of the spliceosome complex C, which mediates the second trans-esterification reaction (Will and Luhrmann 2011). Although the major steps of intron splicing and components of different complexes have been identified, the mechanism and regulation of B-complex activation are not characterized.

Prp4, the only serine/threonine protein kinase among the spliceosome components, plays a critical role in the activation of B-complex in humans and fission yeast *Schizosaccharomyces pombe* (Fair and Pleiss 2017; Bottner et al. 2005; Schneider et al. 2010). It functionally interacts with Prp6, Prp31, Brr2, and Prp8 proteins of tri-snRNP (Bottner et al. 2005) and Prp4-phosphorylation sites have been identified in Prp6 and Prp31 (Schneider et al. 2010). Both in human and yeast tri-snRNP, Prp31 and Prp6 are at the linker region between U5 and U4/U6 snRNPs (Agafonov et al. 2016; Wan et al. 2016a). Prp31 was first identified in a screen for temperature sensitive mutants with splicing defects at low temperature in the budding yeast *Saccharomyces cerevisiae* (Weidenhammer et al. 1996). As a U4/U6 protein, Prp31 is an essential splicing factor and it has the well-conserved coiled-coil and NOP domains and a less-conserved Prp31_C domain (Gao et al. 2016; Makarova et al. 2002). It mediates the formation of the U4/U6–U5 tri-snRNP by specifically interacting with the U5 protein Prp6 (Agafonov et al. 2016; Makarova et al. 2002) and plays a crucial role in the subsequent spliceosome formation and activation (Schneider et al. 2010). In humans, the NOP domain of Prp31 interacts with both U4 RNA and the 15.5 K protein and reinforces their interaction. Mutations in the coiled-coil and NOP domains are related to human retinitis pigmentosa (RP) and one of these mutations in Prp31 disrupts its interaction with Prp6 (Liu et al. 2007; Vithana et al. 2001), further indicating its importance in the spliceosome.

In humans, Prp31 is also connected to the DExD/H-box family RNA helicase Brr2 by Prp6 (Agafonov et al. 2016). Brr2, a U5 snRNP protein, recognizes the single-stranded region of U4 next to stem I of U4/U6 (Mozaffari-Jovin et al. 2012) and catalyzes the unwinding of U4/U6, which is a critical step of spliceosome activation. In *S. cerevisiae*, Prp31 is dispensable for tri-snRNP formation but promotes the association of tri-snRNP with the prespliceosome during spliceosome maturation (Weidenhammer et al. 1997). The coiled-coil domain of Prp31 contacts the RT domain of Prp8, which like Brr2, is a U5 snRNP protein and plays a key role in spliceosome activation and formation of the catalytic core (Galej et al. 2013; Nguyen et al. 2015). A number of suppressors of yeast U4-cs1 mutant that is defective in the U4/U6 unwinding are at the RT domain of Prp8 (Galej et al. 2013). Prp8 prevents pre-mature U4/U6 unwinding by blocking the loading of Brr2 onto the U4 snRNP (Mozaffari-Jovin et al. 2012) and inserting its C-terminal tail into the RNA binding tunnel of Brr2 (Mozaffari-Jovin et al. 2013). In in vitro U4/U6 unwinding assays, Prp31 also is inhibitory to the helicase activity of Brr2 (Theuser et al. 2016). The position of Prp31 in the tri-snRNP and its interaction with Brr2 and Prp8 suggest an important role of Prp31 in the spliceosome in B-complex activation. In humans, Prp31 is phosphorylated by Prp4, which is required for the stable association of the tri-snRNP with prespliceosome (Schneider et al. 2010). Putative Prp4-phosphorylation sites have been identified in the C-terminal region of human Prp31 by phosphoproteomics analysis (Schneider et al. 2010).

In a previous study, we showed that, unlike its orthologs in *S. pombe*, the FgPrp4 kinase is not essential for viability in *Fusarium graminearum*, which is the major causing agent of Fusarium head blight (FHB), one of the most important diseases of wheat and barley worldwide (Figueroa et al. 2017; Goswami et al. 2006; Jiang et al. 2016). However, the *Fgprp4* deletion mutant had severe defects in intron splicing and growth and often produced spontaneous suppressors with faster growth rate (Gao et al. 2016). Among the nine suppressor strains analyzed, two had mutations in the C-terminal region of Prp31. One of them had a nonsense mutation at R464 that resulted in the truncation of the C-terminal 130 aa residues of FgPrp31, including residue L532 that was changed to P in the other suppressor (Gao et al. 2016). To further characterize the function of FgPrp31 and its relationship with FgPrp4 kinase, in this study we identified 26 additional suppressor mutations in the C-terminal 465–594 aa region (CT130) of FgPrp31 that contains all the putative Prp4-phosphorylation sites reported in humans. The CT130 of FgPrp31 displayed self-inhibitory interaction with its N-terminal 1–463 aa region (N463) that directly interacted with FgPrp6 and FgBrr2. Truncation or point mutations in FgPrp31 abolished its self-inhibitory binding, decreased its interaction with FgPrp6, but increased its interaction with FgBrr2. Site-directed mutagenesis analysis showed that mutations at multiple phosphorylation sites are necessary to suppress *Fgprp4*, and the S520 and S521 residues of FgPrp31 are likely important Prp4 phosphorylation sites. These results indicated that phosphorylation of Prp31 by Prp4 at multiple sites may release its self-inhibitory binding and affect the interaction of FgPrp31 with other components of tri-snRNP during spliceosome activation.

Results

Suppressors S2 is only partially recovered in intron splicing efficiency

Suppressor S2 of the *Fgprp4* mutant had a nonsense mutation at R464 (R464*) in *FgPRP31* that resulted in the truncation of its CT130 region (Fig. 1a). However, although it was recovered in growth rate, suppressor S2 was still

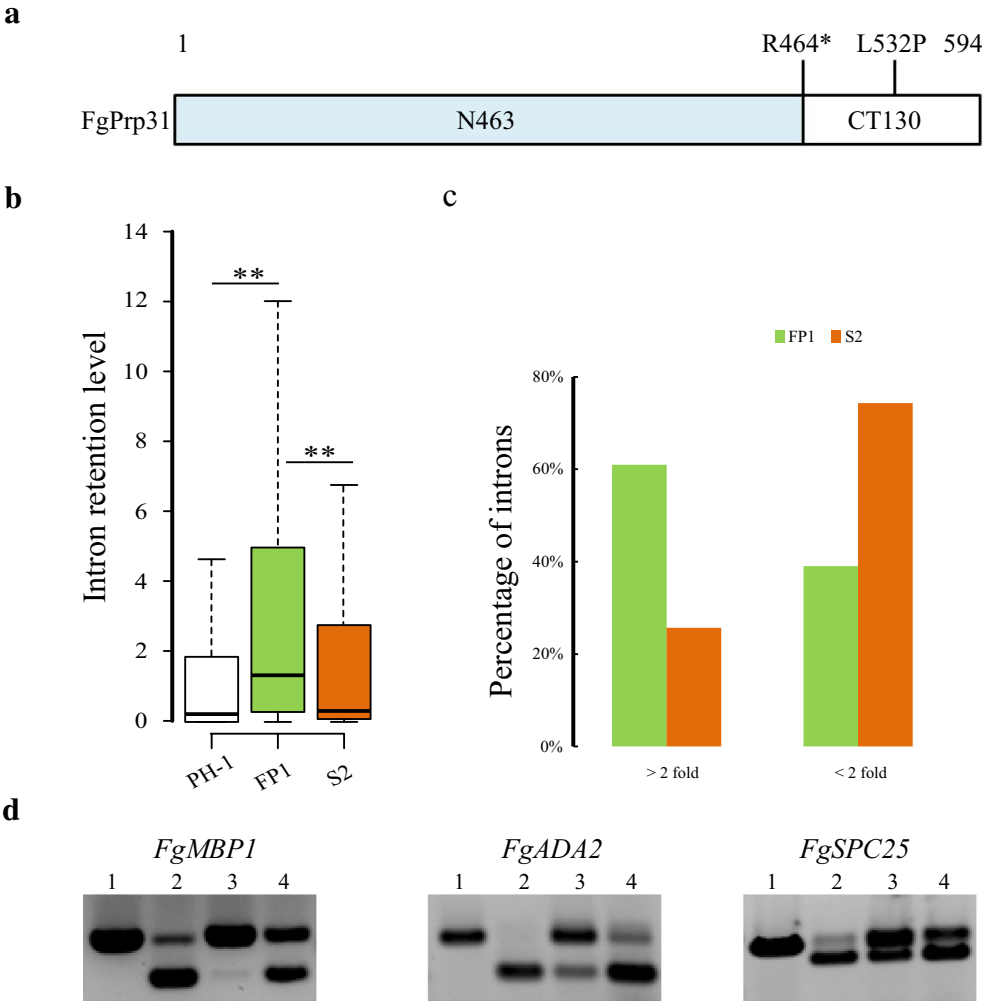

Fig. 1 Intron splicing defects of suppressor S2 with the R464* mutation in *FgPRP31*. **a** Schematic drawing of FgPrp31 with the marked R464* and L532P mutations. N463 and CT130 refers to the N-terminal 463-aa and C-terminal 130-aa regions of FgPrp31, respectively. **b** Box-plot comparison of intron retention levels in the wild type (PH-1), *Fgprp4* mutant (FP1), and suppressor S2. The statistical significance for each comparison is analyzed by *t* test (**$P < 0.01$). The intron retention level was defined as the number of reads that aligned to the predicted intron divided by the number of reads aligned to the corresponding transcript. **c** The percentage of introns with the over or less than twofold increase in the intron retention level in *Fgprp4* mutant FP1 and suppressor S2 in comparison with the wild-type strain PH-1. **d** Intron splicing defects in the labelled genes were verified by RT-PCR. Lanes 1–4 were PCR results with genomic DNA of PH-1 and cDNA of PH-1, *Fgprp4*, and suppressor S2, respectively

impaired in conidiation and plant infection (Gao et al. 2016), suggesting that the R464* mutation only partially rescued the intron splicing defects of *Fgprp4*. To test this hypothesis, we performed RNA-seq analysis with RNA isolated from aerial hyphae of S2. The intron retention level (percentage of un-spliced introns) was still higher in suppressor S2 than that of the wild-type strain PH-1 although it was significantly reduced compared to that of the original *Fgprp4* mutant FP1 (Fig. 1b) (Gao et al. 2016). For the 7414 introns from the 5252 genes that were expressed in all three strains, approximately 61 and 26% of them had over twofold increase in the intron retention level in *Fgprp4* mutant FP1 and suppressor S2, respectively, in comparison with that of PH-1 (Fig. 1c). These results indicate that the R464* mutation in *FgRPP31* only partially rescued the intron splicing defects of *Fgprp4*. Among the genes that still had over twofold higher intron retention level than PH-1 in suppressor S2, a number of them are known to be functionally related to conidiation, pathogenesis, and sexual reproduction, such as *FgMBP1, FgADA2*, and *FgSPC25* (Fig. 1d) (Church et al. 2017; Hendler et al. 2017; Janke et al. 2001), which may be related to its incomplete or partial recovery in phenotypes.

The C-terminal 130 aa region of FgPrp31 is dispensable for its function

The R464* mutation in *FgPRP31* resulted in the truncation of the CT130 region, which includes L532 that was changed to P in suppressor S17 (Fig. 1a). To determine the importance of this CT130 region, we generated the *FgPRP31*$^{\Delta CT130}$ construct in which the 1498–1890 bp fragment (corresponding to 464–594 aa) was replaced with the geneticin (GenR) cassette (Fig S1a) and transformed it into PH-1. Geneticin-resistant transformants were isolated and assayed for the truncation of CT130 by PCR and sequencing analysis. To our surprise, the resulting *FgPRP31*$^{\Delta CT130}$ mutants (Table 1) were normal in hyphal growth, sexual reproduction, and plant infection (Fig S1b), suggesting that this region is not essential for *FgPRP31* function. We then attempted to generate the *Fgprp31* deletion mutant by gene replacement. After screening over hundreds of hygromycin-resistant transformants derived from multiple transformations, we failed to identify *Fgprp31* mutant, suggesting that *FgPRP31*, like its yeast ortholog, is an essential gene in *F. graminearum*.

Table 1 Wild type and transformants of *Fusarium graminearum* strains used in this study

Strain	Brief description	References
PH-1	Wild type	Caomo et al. (2007)
FP1	*Fgprp4* deletion mutant of PH-1	Wang et al. (2011)
S2	Suppressor of FP1 with the R464* mutation in *FgPRP31*	Gao et al. (2016)
S17	Suppressor of FP1 with the L532P mutation in *FgPRP31*	Gao et al. (2016)
S47	Suppressor of FP1 with the R230H mutation in *FgPRP6*	Gao et al. (2016)
Suppressors S50–S309	Spontaneous suppressor strains of mutant FP1	This study
NC1-16	*FgPRP31*^{R463}-3xFLAG *FgPRP31*^{CT130}-GFP transformant of PH-1	This study
DS2-D	*FgPRP31*^{CT130} mutant of PH-1	This study
CICK-1	*FgPRP31*^{R463}-3xFLAG transformant of PH-1	This study
CICK-2	*FgPRP31*^{CT130}-GFP transformant of PH-1	This study
PP31-1	*FgPRP31*-GFP transformant of PH-1	This study
SP31-2	*FgPRP31*-GFP transformant of suppressor S47	This study
AP1, AP2, AP3, AP4, AP5	*Fgprp31 FgPRP31*$^{S485A\ S486A}$-GFP transformants of PH-1	This study
DP1, DP2, DP3,... DP7	*prp4 FgPRP31*$^{S485D\ S486D}$-GFP transformants of PH-1	This study
SD1, SD2, SD3, SD4	*prp4 FgPRP31*^{S520D}-GFP transformants of PH-1	This study
SG1, SG2, SG3, SG4, SG5	*prp4 FgPRP31*^{S521D}-GFP transformants	This study
PM612-2	*prp4 FgPRP31*$^{S520D\ S521D\ T525D}$-GFP transformant	This study
LG4-4	*FgPRP6*-GFP and *FgPRP31*^{WT}-3xFLAG transformant of PH-1	This study
LG6-8	*FgPRP6*-GFP and *FgPRP31*^{N463}-3xFLAG transformant of PH-1	This study
LG10-15	*FgPRP6*-GFP and *FgPRP31*^{G529D}-3xFLAG transformant of PH-1	This study
LG11-17	*FgPRP6*-GFP and *FgPRP31*^{D534G}-3xFLAG transformant of PH-1	This study
CICK-3	*FgPRP6*-GFP transformant of PH-1	This study
CICK-3	*FgPRP31*-GFP transformant of PH-1	This study
BFY1-8	*FgPRP31*^{WT}-YFPN and *FgPRP6*-YFPC transformant of PH-1	This study
BFY1-14	*FgPRP31*^{WT}-YFPN and *FgPRP6*-YFPC transformant of PH-1	This study
BFY2-3	*FgPRP31*^{N463}-YFPN and *FgPRP6*-YFPC transformant of PH-1	This study
BFY2-6	*FgPRP31*^{N463}-YFPN and *FgPRP6*-YFPC transformant of PH-1	This study
BFY3-4	*FgPRP31*^{L532P}-YFPN and *FgPRP6*-YFPC transformant of PH-1	This study
BFY3-7	*FgPRP31*^{L532P}-YFPN and *FgPRP6*-YFPC transformant of PH-1	This study
BFY4-6	*FgPRP31*^{WT}-YFPN and *FgBRR2*-YFPC transformant of PH-1	This study
BFY4-11	*FgPRP31*^{WT}-YFPN and *FgBRR2*-YFPC transformant of PH-1	This study
BFY5-2	*FgPRP31*^{N463}-YFPN and *FgFgBRR2*-YFPC transformant of PH-1	This study
BFY5-5	*FgPRP31*^{N463}-YFPN and *FgFgBRR2*-YFPC transformant of PH-1	This study
BFY6-10	*FgPRP31*^{L532P}-YFPN and *FgBRR2*-YFPC transformant of PH-1	This study
BFY6-18	*FgPRP31*^{L532P}-YFPN and *FgBRR2*-YFPC transformant of PH-1	This study

CT130 of FgPrp31 interacts with its N-terminal region

Because truncation of CT130 suppressed *Fgprp4*, it is possible that this region of FgPrp31 plays a negative role by binding to its N-terminal region or other Prp31-interacting proteins. To test this hypothesis, we cloned the N-terminal 1-463 aa (N463) and C-terminal 465–594 aa (CT130) regions of FgPrp31 into the Matchmaker vectors as the prey and bait constructs, respectively. Yeast transformants carrying the CT130 bait and N463 prey constructs were able to grow on SD-Trp-Leu-His medium and had LacZ activities (Fig. 2a), indicating their direct interaction.

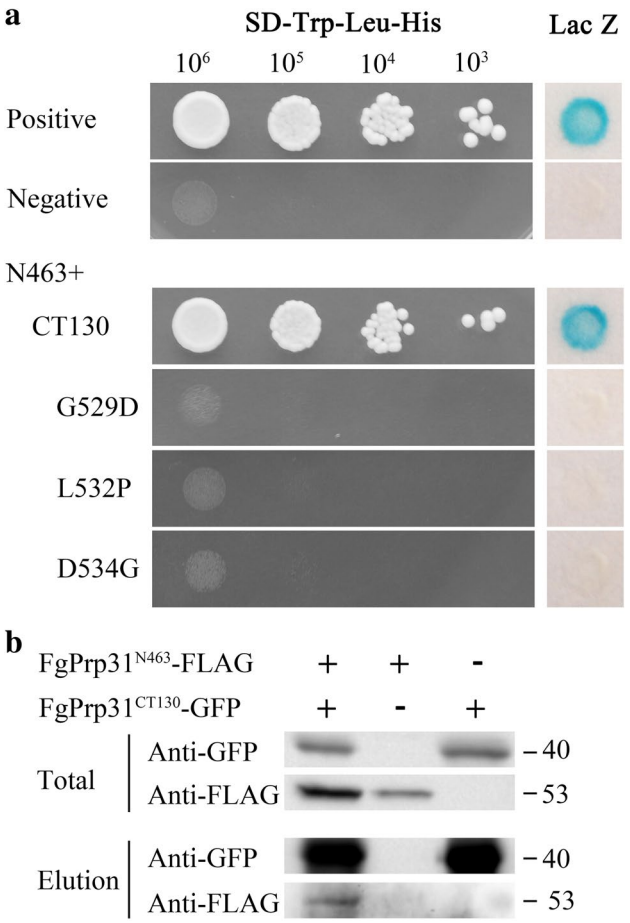

Fig. 2 Interaction between the CT130 and N463 of FgPrp31. **a** Yeast cells expressing the FgPrp31$^{1–463}$ (N463) bait construct and FgPrp31$^{465–594}$ (CT130) prey constructs with or without the labelled point mutations were assayed for growth on SD-Trp-Leu-His plates (left) and LacZ activities (right). The positive and negative controls are from the Matchmaker kit. The interaction between CT130 and N463 was abolished by the G529D, L532P, or D534G mutation. **b** Western blots of total proteins (total) and proteins eluted (elution) from anti-FLAG beads of transformants expressing the *FgPRP31*^{N463}-3×FLAG and/or *FgPRP31*^{CT130}-GFP constructs were detected with an anti-GFP or anti-FLAG antibody

To determine the effect of L532P mutation on the interaction between the N463 and CT130 of FgPrp31, we also generated the CT130^{L532P} bait construct. Yeast cells expressing the N463 prey and CT130^{L532P} bait constructs failed to grow on SD-Trp-Leu-His plates and had no detectable LacZ activities (Fig. 2a), suggesting that the L532P mutation abolished the interaction between CT130 and N463 of FgPrp31. Therefore, the R464* and L532P suppressor mutations may have similar effects on releasing the self-inhibitory binding of the CT130 with N463 of FgPrp31.

To confirm their interaction in vivo, we then generated the *FgPRP31*^{N463}-3×FLAG and *FgPRP31*^{CT130}-GFP constructs and transformed them into PH-1. The resulting transformant NC1-16 (Table 1) were confirmed by PCR and western blot analyses for the expression of transforming constructs. In co-immunoprecipitation (co-IP) assays, a 40-kDa band was detected with the anti-GFP antibody in both total proteins isolated from transformant NC1-16 and proteins eluted from anti-FLAG beads (Fig. 2b). These results confirmed the interaction between the CT130 and N463 regions of FgPrp31.

The R464* and L532P mutations in FgPrp31 increase its interaction with FgBrr2

In yeast and mammalian cells, Prp31 is known to interact with Brr2, Prp6, and other components of the U4/U6–U5 tri-snRNP (Agafonov et al. 2016; Wan et al. 2016b). To determine the effects of R464* mutation, we first assayed the interaction of the full-length FgPrp31^{WT} or truncated FgPrp31 (N463) with FgBrr2. Due to its size, we generated two bait constructs of FgBrr2 that had the 1-872 aa fragment (Brr2N) containing the N-terminal region and the Rec1 domain and 1285–2206 aa fragment (Brr2C) containing the C-terminal helicase cassette. In yeast two-hybrid assays, neither of these two FgBrr2 fragments interacted with the prey construct of FgPrp31^{WT} (Fig. 3a; Fig S2). However, N463 of FgPrp31 interacted with Brr2N (Fig. 3a) but not with Brr2C (Fig S2). These results indicate that the nonsense mutation at R464 enables the interaction of FgPrp31 with the N-terminal region of FgBrr2.

To further verify the effect of R464* mutation, we generated the *FgPRP31*^{WT}-YFPN, *FgPRP31*^{N463}-YFPN, and *FgBRR2*-YFPC constructs and transformed them in pairs into PH-1. In the resulting transformants (Table 1), YFP signals were mainly observed in the nucleus. In comparison with the *FgPRP31*^{WT}-YFPN *FgBRR2*-YFPC transformants, YFP signals were stronger in the *FgPRP31*^{N463}-YFPN *FgBRR2*-YFPC transformants (Fig. 3b), confirming that the nonsense mutation at R464 increased the interaction between FgPrp31 and FgBrr2.

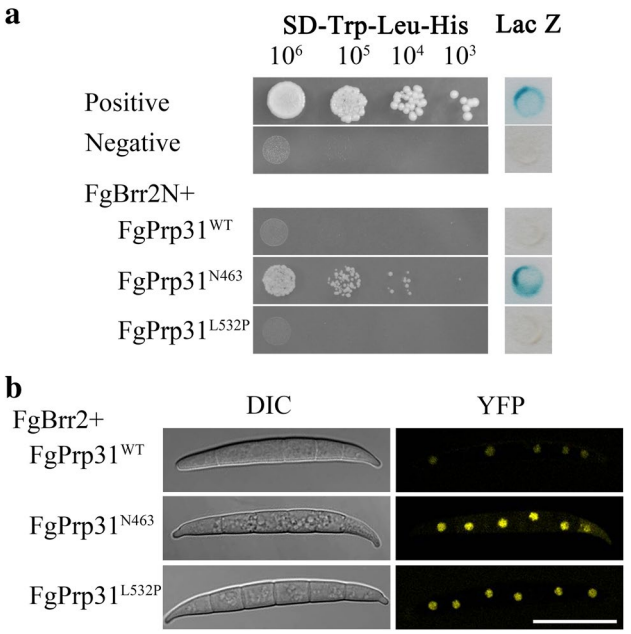

Fig. 3 Assays for the interaction of FgPrp31 with FgBrr2. **a** Yeast two-hybrid assays for the interaction of FgPrp31^{WT}, FgPrp31$^{1–463}$ (N463) or FgPrp31^{L532P} with the N-terminal (Brr2N) region of FgBrr2. Yeast cells expressing the marked bait and prey constructs were assayed for growth on SD-Trp-Leu-His plates (left) and LacZ activities (right). The truncation of C-terminal 130 aa of FgPrp31 enabled the interaction between these two key tri-snRNP components. Positive and negative controls are from the Matchmaker kit. **b** BiFC assays for the interaction between FgPrp31 and FgBrr2. Conidia of transformants expressing the *FgBRR2*-YFPC and *FgPRP31*^{WT}-, *FgPRP31*^{N463}-, or *FgPRP31*^{L532P}-YFPN constructs were examined by DIC and epifluorescence microscopy. Both FgPrp31^{N463} and FgPrp31^{L532P} had stronger interactions with FgBrr2 than FgPrp31^{WT}. Bar 20 μm

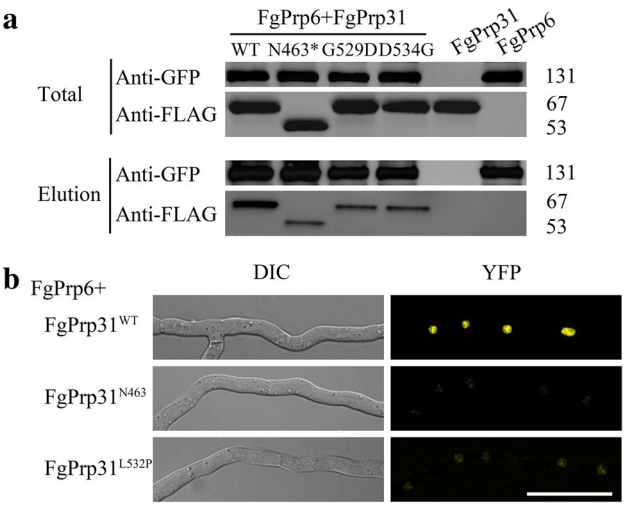

Fig. 4 Co-IP and BiFC assays for the interaction between FgPrp31 and FgPrp6. **a** Western blots of total proteins and proteins eluted from anti-GFP beads of transformants expressing the *FgPRP6*-GFP and *FgPRP31*^{WT}-, *FgPRP31*^{N463}-, *FgPRP31*^{D534G}-, or *FgPRP31*^{G529D}-3×FLAG fusion constructs were detected with an anti-GFP or anti-FLAG antibody. The nonsense mutation at R464 and G529D or D534G mutation reduced the interaction of FgPrp6 with FgPrp31. **b** Hyphae of transformants expressing the FgPrp6-YFPC and FgPrp31^{WT}-, FgPrp31^{N463}-, or FgPrp31^{L532P}-YFPN constructs were examined by DIC and epifluorescence microscopy. YFP signals were weaker in transformants expressing the mutant alleles of *FgPRP31*. Bar 20 μm

We also generated the prey construct of the full-length FgPrp31 carrying the L532P mutation. In yeast two-hybrid assays, FgPrp31^{L532P} failed to interact with Brr2N or Brr2C (Fig. 3a; Fig S2). Interestingly, the *FgPRP31*^{L532P}-YFPN *FgBRR2*-YFPC transformants also had stronger YFP signals than the *FgPRP31*^{WT}-YFPN *FgBRR2*-YFPC transformants (Fig. 3b). These results indicate that although it had no obvious effect in yeast two-hybrid assays, the L532P mutation in FgPrp31 also increased its interaction with FgBrr2 in vivo, possibly due to their enhanced associations with other tri-snRNP components in *F. graminearum*.

Truncation of CT130 in FgPrp31 reduces its interaction with FgPrp6

Prp6 and Prp31 are two key components of the U4/U6–U5 tri-snRNP that are known to interact with each other (Liu et al. 2006, 2007). To our surprise, we failed to observe the interaction between FgPrp6 and FgPrp31^{WT}, N463 of FgPrp31, or FgPrp31^{L532P} in yeast two-hybrid assays (Fig S2). To assay their interactions in vivo, we generated the *FgPRP6*-GFP and *FgPRP31*-3×FLAG fusion constructs and transformed them into the wild-type strain PH-1. In the resulting transformants expressing both *FgPRP6*-GFP and *FgPRP31*^{WT}-3×FLAG constructs (Table 1), the 67-kDa FgPrp31-3×FLAG band was detectable in total proteins and proteins eluted from anti-GFP beads (Fig. 4a). To verify their interactions by BiFC assays, we also generated the *FgPRP6*-YFPC construct and co-transformed it with *FgPRP31*^{WT}-YFPN into PH-1. In the resulting transformants (Table 1), YFP signals were observed in the nucleus (Fig. 4b), indicating the interaction of FgPrp6 with FgPrp31 in *F. graminearum*.

To determine the effect of nonsense mutation at R464 on their interaction, we generated the *FgPRP31*^{N463}-3×FLAG construct and co-transformed it with *FgPRP6*-GFP into PH-1. In the resulting transformants, the 53-kDa FgPrp31^{N463}-3×FLAG band was detectable in total proteins and proteins eluted from anti-GFP beads. However, in comparison with the *FgPRP31*^{WT} transformants, the *FgPRP31*^{N463} transformants had a much weaker FLAG band in proteins eluted from anti-GFP beads (Fig. 4a). In BiFC assays, the *FgPRP31*^{N463}-YFPN *FgPRP6*-YFPC and *FgPRP31*^{L532P}-YFPN *FgPRP6*-YFPC transformants

also had weaker YFP signals than the *FgPRP31*^{WT}-YFPN *FgPRP6*-YFPC transformants (Fig. 4b). These results suggested that the truncation of CT130 by R464* mutation reduced the interaction of FgPrp31 with FgPrp6.

Identification of additional suppressor mutations in *FgPRP31*

To better understand suppressor mutations in *FgFRP31*, we isolated 260 additional type I suppressors of the *Fgprp4* mutant that were recovered in growth rate as described in an earlier study (Gao et al. 2016) (Table 1). After sequencing its coding region, a total of 33 additional suppressor strains with mutations in *FgPRP31* were identified (Table 2). Whereas seven of them had suppressor mutations in the N-terminal region (7–64 aa) of *FgPRP31*, the other 26 suppressors had missense or nonsense mutations at nine different sites in the CT130 region (Fig. 5a), including one additional L532P and three additional R464* mutations. A total of 19 suppressor strains had either missense or nonsense mutations between L522 and Q538, including five suppressors with the Q528* and six with the D534G mutations (Table 2).

When six suppressor strains with the L522P, G529D, L532P, D534G, P535S, or Q538* mutation were assayed, they all had similar phenotypes as S2 and S17 in growth and sexual reproduction (Fig. 5b). In yeast two-hybrid assays, the G529D or D534G mutation had the same effects with L532P mutation in eliminating the interaction between CT130 and N463 of FgPrp31 (Fig. 2a), suggesting that these suppressor mutations likely affect the inhibitory binding of FgPrp31^{CT130}. In co-IP assays, the D534G and G529D mutations also reduced the interaction of FgPrp31 with FgPrp6 (Fig. 4a). These results further indicate that the CT130 of FgPrp31 is involved in the negative regulation of its functions.

The N-terminal 225 aa of FgPrp31 is important for interacting with CT130

Interestingly, the D7N, D11N, and Δ11–64 mutations identified in seven suppressor strains (Fig. 5a) occurred between residues 7 to 64 of FgPrp31. To determine whether this 7–64 aa fragment functions as the interacting site with CT130 of FgPrp31, we generated the FgPrp31$^{1–75}$, FgPrp31$^{1–225}$, and FgPrp31$^{76–225}$ prey constructs. In yeast two-hybrid assays, both FgPrp31$^{1–225}$ and FgPrp31$^{76–225}$, but not FgPrp31$^{1–75}$, interacted with CT130 (Fig. 5c). Therefore, the 76–225 aa region of FgPrp31, but not the first 75 aa, likely plays a critical role in interacting with CT130. The D7N, D11N, or Δ11–64 mutation may affect the conformation or structure of the CT130-interacting region of FgPrp31.

FgPrp31 is phosphorylated by FgPrp4 in *F. graminearum*

To determine whether FgPrp31 is phosphorylated by FgPrp4 kinase, we transformed the *FgPRP31*-GFP construct under the control of RP27 constitutive promoter into the wild-type PH-1 and suppressor S47 (*Fgprp4 FgPRP6*^{R230H}). Suppressor S47 was used instead of the original *Fgprp4* mutant because of its slow growth rate and instability (Gao et al. 2016). In western blot analysis with proteins eluted from anti-GFP beads, similar expression levels of FgPrp31-GFP was

Table 2 Mutations in *FgPRP31* identified in spontaneous suppressors of *Fgprp4*

Suppressor strain	Nucleotide change	Amino acid changes
S2	C^{1498}GA to TGA	R464*[a] (TGA)
S17	CT^{1703}C to CCC	L532P
S57	C^{1720}AG to TAG	Q538*[a]
S98	Δ33–192	Δ11–64
S109, S208, S224	C^{1498}GA to TGA	R464*[a]
S110	CT^{1703}C to CCC	L532P
S113, S169, S226 S233, S289	C^{1690}AG to TAG	Q528*[a]
S141	C^{1711}CC to TCC	P535S
S158, S175, S216, S229, S237, S306	GA^{1709}T to GGT	D534G
S182, S244, S254, S263 S282	TGG^{1530} to TGA	W474*[a]
S206, S214, S231, S305	G^{31}AT to AAT	D11N
S213, S223, S270	GG^{1694}T to GAT	G529D
S243, S299	G^{19}AT to AAT	D7N
S307	CT^{1673}G to CCG	L522P

[a]*Refers to stop codon

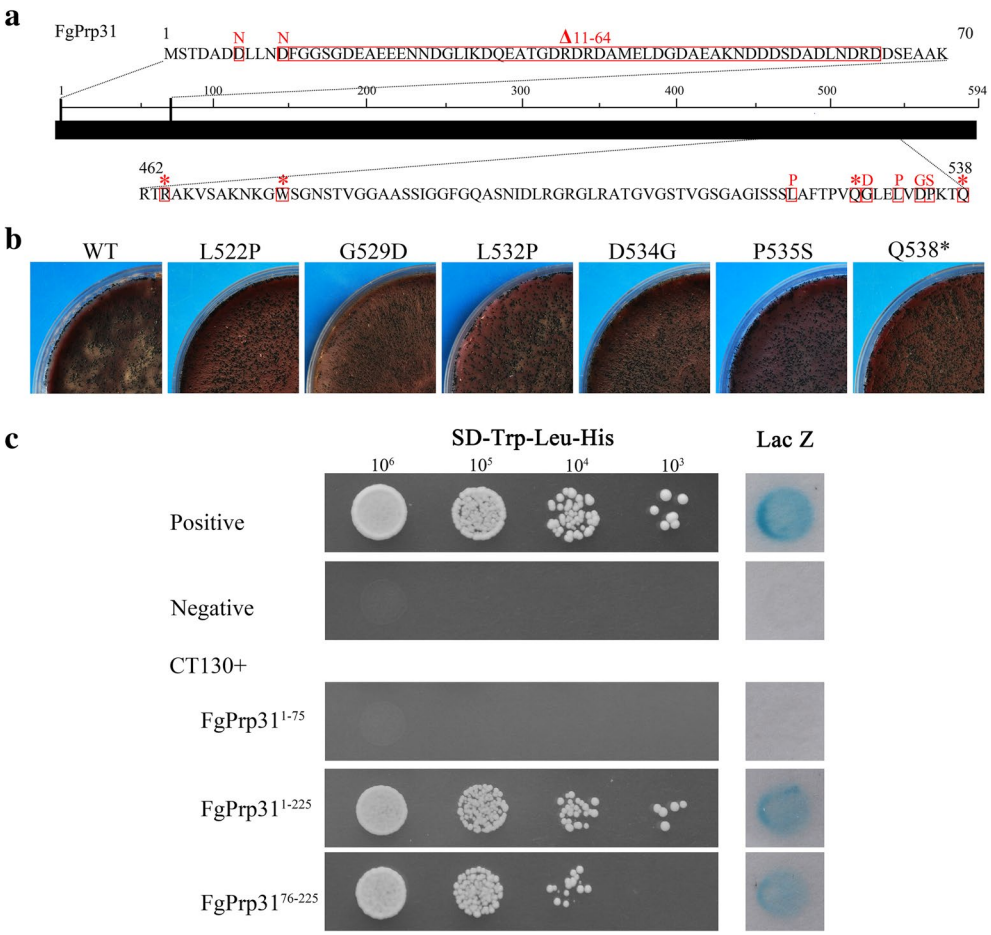

Fig. 5 Additional suppressor mutations identified in *FgPRP31*. **a** Thirty-three additional suppressor strains had mutations in the N-terminal region (upper) and C-terminal region (lower) of *FgPRP31*. The suppression mutations were labeled on the top of the boxed mutation sites. **b** Mating plates of suppressor strains carrying the marked suppressor mutations in *FgPRP31*. **c** Yeast two-hybrid assays for the interaction between the C-terminal 130 aa of FgPrp31 (CT130) with its N-terminal 1–75, 1-225, or 76–225 aa regions

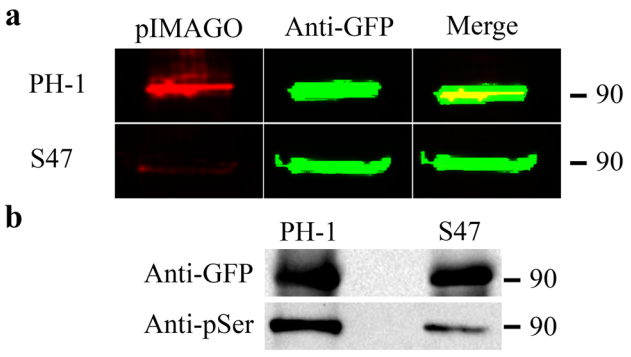

Fig. 6 Phosphorylation assays with FgPrp31-GFP fusion proteins. Total proteins were isolated from transformants of the wild-type strain PH-1 or suppressor S47 (*Fgprp4 FgPRP6*^{R230H}) expressing the *FgPRP31*-GFP fusion construct. **a** Western blots of proteins eluted from anti-GFP beads were detected for the expression of FgPrp31-GFP fusion with an anti-GFP antibody (false color green) and for its phosphorylation with pIMAGO (false color red). **b** Western blots of proteins eluted from anti-GFP beads were detected with an anti-GFP or anti-pSer antibody

detected in transformants of PH-1 and S47 (Fig. 6a). However, when detected for phosphorylation with the pIMAGO reagent, the Prp31-GFP band was much stronger in the wild type than in S47 (Fig. 6a), indicating that phosphorylation of FgPrp31 was significantly reduced in the *Fgprp4* mutant.

To confirm this observation, western blots of proteins eluted from anti-GFP beads were also detected with an anti-phosphoserine antibody. In comparison with that of the wild type, the phosphorylation level of FgPrp31 at Ser residues was reduced in suppressor S47 (Fig. 6b), which also suggested that FgPrp31 is phosphorylated by FgPrp4 in *F. graminearum*.

S520A S521A T525A mutation may be lethal but S485A S486A mutation has no significant effects on FgPrp31 functions

Sequence alignment showed that the CT130 region of FgPrp31 is not well conserved among its orthologs from yeast, filamentous fungi, plants, and animals. Interestingly,

five of the Prp4-phosphorylation sites identified in human Prp31 are conserved in FgPrp31 (S485, S486, S520, S521, and T525) and its orthologs from other filamentous ascomycetes. To determine their roles in FgPrp31 activation, we first generated the *FgPRP31*$^{S485A\ S486A}$-GFP and *FgPRP31*$^{S520A\ S521A\ T525A}$-GFP (GenR) alleles and co-transformed them individually with the *FgPRP31* knockout construct (HygR) into PH-1. Mutants resistant to both geneticin and hygromycin were screened by PCR for deletion of *FgPRP31*. The *Fgprp31* deletion mutants were then examined for GFP signals. In total, five *Fgprp31 FgPRP31*$^{S485A\ S486A}$-GFP transformants (Table 1) were identified. They were similar to the wild type in growth rate (Fig. 7a) and conidiation (Fig. 7b) and had GFP signals in the nucleus (Fig. 7c). However, we failed to identify *Fgprp31 FgPRP31*$^{S520A\ S521A\ T525A}$-GFP transformants after screening over 100 transformants. Because *FgPRP31* is likely an essential gene, these results indicated that the S485A S486A mutation had no significant effects on *FgPRP31* functions but the S520A S521A T525A mutation may be lethal in *F. graminearum*. Therefore, residues S520, S521, and T525 may be important FgPrp4-phosphorylation sites in FgPrp31.

S520D and/or S521D are suppressive to the *Fgprp4* mutant

We also generated the *FgPRP31*$^{S485D\ S486D}$-GFP and *FgPRP31*$^{S520D\ S521D\ T525D}$-GFP alleles and co-transformed them with the *PRP4* knockout construct (Wang et al. 2011) into PH-1. Transformants resistant to both hygromycin and geneticin were first screened for deletion of *FgPRP4*. The *Fgprp4* deletion mutants were then examined for GFP signals in the nucleus. Seven *prp4 FgPRP31*$^{S485D\ S486D}$-GFP transformants (Table 1) with similar colony morphology were identified. In comparison with the wild type, their growth rate was significantly reduced but they still grew slightly faster than *Fgprp4* (Fig. 7a). Conidiation also was only slightly higher in *prp4 FgPRP31*$^{S485D\ S486D}$-GFP transformants than in *Fgprp4* (Fig. 7b). In contrast, the *prp4 FgPRP31*$^{S520D\ S521D\ T525D}$-GFP transformants grew as fast as the wild type (Fig. 8a) and were normal in conidiation (Fig. 8b). These results suggest that the S485D S486D mutations had only minor effects but S520D S521D T525D mutations in *FgPRP31* could suppress the defects of *Fgprp4* in growth and conidiation, further indicating the importance of S520, S521, and T525 as Prp4-phosphorylation sites in *F. graminearum*.

To determine which residue is more critical, we introduced the S520D, S521D, or T525D mutation into the *FgPRP31*-GFP construct. The resulting mutant alleles of *FgPRP31* were co-transformed with the *PRP4* knockout cassette (Wang et al. 2011) into PH-1. Whereas we failed to isolate *Fgprp4 FgPRP31*^{T525D}-GFP transformants, four *prp4 FgPRP31*^{S520D}-GFP and five *prp4 FgPRP31*^{S521D}-GFP transformants (Table 1) were identified by PCR and found to have GFP signals in the nucleus. They all grew slower than the wild type but much faster than the *Fgprp4* mutant (Fig. 8a). The *prp4 FgPRP31*^{S521D}-GFP and *prp4 FgPRP31*^{S520D}-GFP transformants also produced more conidia than *Fgprp4* but not to the wild-type level (Fig. 8b). These results suggested that the S520D or S521D mutation in *FgPRP31* could partially suppress the *Fgprp4* mutant. It

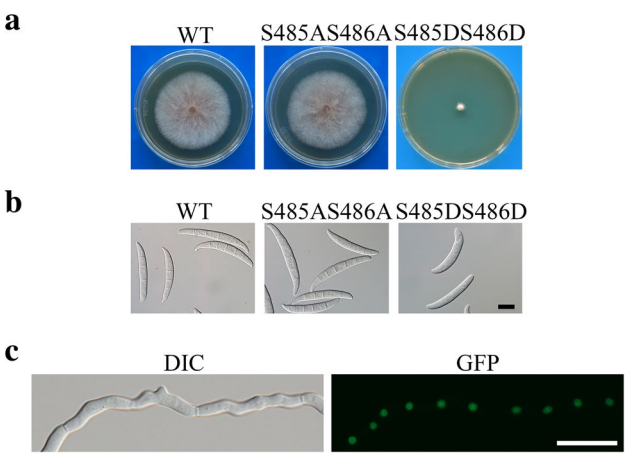

Fig. 7 Site-directed mutagenesis of S485 and S486 in *FgPRP31*. **a** Three-day-old PDA cultures of the wild-type strain and the *Fgprp31*/*FgPRP31*^{S485AS486A}-GFP and *Fgprp4*/*FgPRP31*$^{S485D\ S486D}$-GFP transformants. **b** Conidiation in 5-day-old CMC cultures of the same set of strains. Bar 10 μm. **c** GFP signals were observed in the nucleus in the *Fgprp31*/*FgPRP31*$^{S485A\ S486A}$-GFP transformant. Bar 20 μm

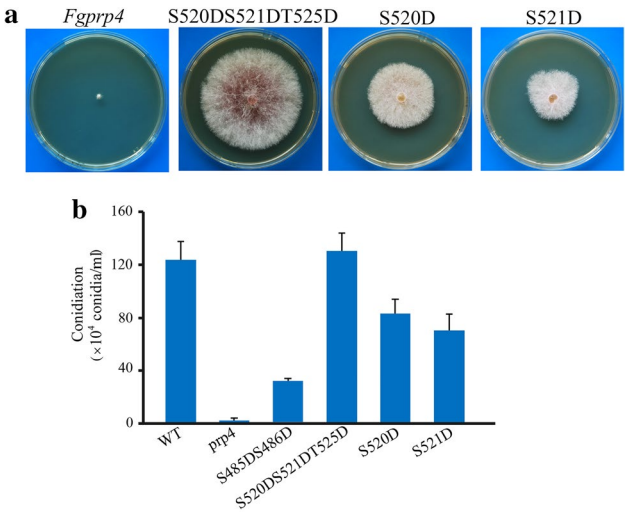

Fig. 8 Site-directed mutagenesis of putative phosphorylation sties in *FgPRP31*. **a** Three-day-old PDA cultures of the *Fgprp4* mutant and transformants of *Fgprp4* mutant expressing the labelled mutant alleles of *FgPRP31*. **b** Conidiation in 5-day-old CMC cultures of the wild type, *Fgprp4* mutant, and the same set of strains as in **a**

is likely that phosphorylation at multiple sites, particularly at S520 and S521, is necessary for normal FgPrp31 functions.

Discussion

Protein phosphorylation plays important roles in modulating the assembly and disassembly of snRNPs during the catalytic cycle of the spliceosome (McKay and Johnson 2010). In humans, phosphorylation of Prp31 and Prp6 by Prp4 kinase occurs concomitantly with the stable integration of tri-snRNP into A-complex (Schneider et al. 2010), possibly during pre-B to B-complex transition (Boesler et al. 2016). In *S. pombe*, phosphorylation of Prp1 (Prp6 in human) by Prp4 kinase controls the formation of a competent U4/U6–U5 tri-snRNP for being integrated into spliceosome or B-complex activation (Kuhn and Kaufer 2003). However, the detailed molecular mechanism for the contribution of Prp4 phosphorylation to snRNP remodeling is not fully understood. Our previous work identified mutations in *FgPRP31* in two spontaneous suppressors of the *Fgprp4* mutant in *F. graminearum* (Gao et al. 2016). In this study, we identified 33 additional spontaneous mutations in *FgPRP31* that suppressed the *Fgprp4* mutant. Majority of these suppressor mutations occurred in the vicinity of the five putative Prp4-phosphorylation sites that are conserved in FgPrp31 and its orthologs from human and other filamentous fungi. It is possible that these mutations may have similar effects on FgPrp31 proteins as phosphorylation by FgPrp4 during vegetative growth.

As one of the key components of the U4/U6–U5 tri-snRNP, Prp31 is essential for spliceosome function and intron splicing (Makarova et al. 2002; Weidenhammer et al. 1996). In comparison with Brr2 and Prp8, two other important tri-snRNP components, Prp31 is less conserved in filamentous fungi. In *S. cerevisiae*, the *prp31*-1^{ts} allele is synthetic lethal with cold-sensitive U4-cs1 mutation, indicating a positive function of Prp31 in spliceosome activation (Kuhn et al. 2002). In humans, Prp31 interacts with Prp6, another tri-snRNP protein, in its coiled-coil region (parts of the NOSIC and NOP domains) (Liu et al. 2007). Mutations in this region affecting the interaction of Prp31 with Prp6 caused retinitis pigmentosa and pre-mRNA splicing defects (Vithana et al. 2001), suggesting the importance of the Prp6–Prp31 interaction. Consistently, none of the suppressor mutations identified in *FgPRP31* is in this important Prp6-interacting region. In fact, 26 out of 33 suppressor mutations identified in this study are in the CT130 region of FgPrp31 that is not well conserved among its orthologs. Unfortunately, it is impossible to predict the effects of these suppressor mutations on FgPrp31 structure because crystallography structure is only available for the N-terminal portion of Prp31 (Liu et al. 2007).

Our results showed that the CT130 of FgPrp31 had the inhibitory binding with its N-terminal 76–225 aa region. Among the 28 suppressor mutations identified in this CT130 region, 15 were nonsense mutations and the others were point mutations between L522 and Q538, including the G529D, L532P, and D534G mutations that were shown to eliminate the interaction of CT130 with $FgPrp31^{N463}$. It is possible that all these suppressor mutations in FgPrp31 affected its intra-molecular interaction. Considering the location of the five putative Prp4-phosphorylation sites, it is tempting to hypothesize that phosphorylation by FgPrp4 may result in structural changes of FgPrp31 and releasing its self-inhibitory binding between CT130 and $FgPrp31^{N463}$ in *F. graminearum*. In fact, in human spliceosomal B-complex, the phosphorylated form of Prp31 has an extended conformation and its C-terminal tail does not contact with the N-terminal coiled-coil and NOP domains (Bertram et al. 2017; Boesler et al. 2016). In *S. cerevisiae* that lacks the Prp4 kinase, Prp31 likely lacks the self-inhibitory binding because it has a shorter C-terminal region, which is similar to truncated FgPrp31 in *F. graminearum*. The Prp31 orthologs from other yeast species lacking Prp4 orthologs also have a shorter C-terminal region than FgPrp31.

Considering the importance of the CT130 of FgPrp31 in suppressing *Fgprp4*, it was surprising that deletion of this region alone had no obvious effects on vegetative growth, reproduction, and pathogenesis in *F. graminearum*. It is possible that the basic functions of FgPrp31 in the spliceosome and intron splicing depend on the region conserved between yeast and filamentous fungi and CT130 has no other function but the self-inhibitory binding with $FgPrp31^{N463}$. Recently, deletion of *MoSFL1* was shown to suppress the growth defects of the *cpk1cpk2* deletion mutant although the *Mosfl1* deletion mutant was normal in growth in the rice blast fungus *Magnaporthe oryzae* (Li et al. 2017). The MoSfl1 functions as a repressor that requires phosphorylation by PKA to release its suppression of genes important for hyphal growth via the Cyc8-Tup1 co-repressor (Li et al. 2017). Nevertheless, it remains possible that truncation of the CT130 of *FgPRP31* has cost effects on the survival of *F. graminearum* in nature or other phenotypes that could not be assayed under laboratory conditions.

Interestingly, three suppressor mutations, D7N, D11N, and deletion of 11–64 aa, are in the N-terminal head region of FgPrp31 (D7–D64), which prompted us to hypothesize that this region of FgPrp31 directly interacts with the CT130. However, yeast two-hybrid assays showed that the 76–225 aa region of FgPrp31, not the D7–D64 region, interacted with CT130. Interestingly, the D7–D64 region of FgPrp31 is aspartic acid (D)-rich (29%). It is possible that the D7N and D11N mutations and deletion of D11-D64 affect the structure of the N-terminal region of FgPrp31, which may in turn affect the self-inhibitory binding between the 76–225

aa region and CT130. It is also possible that mutations in the 7–64 aa region of FgPrp31 may affect its association with U4/U6 in *F. graminearum*. Nevertheless, no suppressor mutations of *Fgprp4* were identified in the 76–225 aa region of FgPrp31 that has the coiled-coil domain. In humans, the coiled-coil domain of Prp31 interacts with Sad1 in tri-snRNP (Agafonov et al. 2016) and with the RT domain of Prp8 in the B-complex (Bertram et al. 2017). Considering its importance for interacting with other tri-snRNP components, mutations in this region of *FgPRP31* may be lethal or detrimental to growth in *F. graminearum*. The binding of CT130 to the 76–225 aa region of FgPrp31 likely functions to compete or interfere with its interaction with other tri-snRNP proteins.

Due to its size, we broke FgBrr2 into two fragments for assaying its interaction with FgPrp31 by yeast two-hybrid assays. Whereas no interaction was observed between the C-terminal half of FgBrr2 and FgPrp31, its N-terminal fragment (FgBrr2$^{1–872}$) directly interacted with FgPrp31^{N463} but not FgPrp31^{WT}. The self-inhibitory binding of full-length FgPrp31^{WT} may prevent its interaction with FgBrr2. Interestingly, the R464* mutation in FgPrp31 enhanced its interaction with FgBrr2 in yeast two-hybrid assays. In yeast, the N-terminal region of Brr2 auto-inhibits its activity and prevents the premature tri-snRNP dissociation (Absmeier et al. 2015). In *F. graminearum*, the increased interaction between FgPrp31 (a U4/U6 protein) and FgBrr2 (a U5 protein) by these suppressor mutations may affect the auto-inhibition of FgBrr2 and stability of the U4/U6–U6 tri-snRNP. It is possible that phosphorylation by FgPrp4 releases the auto-inhibition of FgPrp31, which in turn enhances its interaction with FgBrr2 in the tri-snRNP during the activation of B-complex.

Although Prp6 is known to interact with Prp31 in other organisms, we failed to detect their interactions in yeast two-hybrid assays. Nevertheless, the interaction between FgPrp6 and FgPrp31 was confirmed by co-IP and BiFC assays in *F. graminearum*. The R464* truncation and L532P, G529D, and G534G point mutations all reduced the interaction of FgPrp31 with FgPrp6 in BiFC assays or co-IP assays. In human tri-snRNP, the interaction between Prp31 and Prp6 mediates the formation of the U4/U6–U5 tri-snRNP (Agafonov et al. 2016; Makarova et al. 2002). It is possible that reduced interaction between FgPrp6 and FgPrp31 may affect their interactions with FgBrr2 or FgPrp8 and facilitate B-complex activation.

Although protein phosphorylation assays showed that FgPrp31 is likely phosphorylated by FgPrp4, none of the suppressor strains we sequenced had mutations in the five putative FgPrp4-phosphorylation sites. It is possible that phosphorylation by FgPrp4 at multiple phosphorylation sites is necessary to activate FgPrp31, and a single mutation at any one of these phosphorylation sites is not sufficient to suppress or only partially suppress *FgPRP4* deletion. Site-directed mutagenesis studies showed that the S520D S521D T525D but not S485D S486D mutations in *FgPRP31* recovered the growth rate and conidiation of *Fgprp4* to the wild-type level. Because *Fgprp31/FgPRP31*$^{S485A\ S486A}$-GFP transformants had no obvious defects and we failed to isolate *Fgprp31/FgPRP31*$^{S520A\ S521A\ T525A}$-GFP transformants, it is likely that S520, S521, and T525 are important FgPrp4-phosphorylation sites in *FgPRP31*. Further characterization showed the S520D or S521D, but not T525D, mutation in *FgPRP31* could partially recovered the growth and conidiation defects of *Fgprp4*, which is similar to the phenotypes of type II suppressors (Gao et al. 2016). Therefore, S520 and S521 are likely the main FgPrp4-phosphorylation sites in FgPrp31. If additional type II suppressor strains were isolated and sequenced in the future, suppressor mutations at some of these conserved phosphorylation sites may be identified in *FgPRP31*. Overall, our results showed that phosphorylation at multiple sites by FgPrp4 kinase may release the self-inhibitory binding between the CT130 and N463 of FgPrp31, which may in turn affect the interaction of FgPrp31 with FgBrr2, FgPrp6, or other tri-snRNP components. Considering its importance for the protein–protein interactions in tri-snRNP, further characterization of FgPrp31 phosphorylation by FgPrp4 and its effects on the tri-snRNP structure will be important for better understanding of B-complex activation and the regulatory role of FgPrp4 in pre-mRNA splicing.

Materials and methods

Culture conditions and plant infection assays

The wild-type strain PH-1, *Fgprp4* mutant and its suppressor strains, and all the transformants generated in this study were cultured on potato dextrose agar (PDA) or complete medium (CM) at 25 °C and assayed for growth rate, conidiation, conidium morphology, and sexual reproduction as described (Hou et al. 2002; Yang et al. 2015). For protoplast preparation and PEG-mediated transformation (Kazi et al. 2017; Zhou et al. 2011a), 300 μg/ml Hygromycin B (CalBiochem, La Jolla, CA, USA) or 400 μg/ml geneticin (Sigma-Aldrich, St. Louis, MO, USA) were added to the regeneration medium for selection. Infection assays with wheat heads and coleoptiles were conducted as described (Liu et al. 2015). Head blight symptoms were examined 14 days post-inoculation (dpi). Infectious hyphae developed in wheat coleoptiles were examined 9 days post-inoculation (dpi).

RNA-seq analysis

Vegetative hyphae of suppressor S2 were harvested from 5-day-old PDA cultures and used for RNA isolation with the TRIzol Reagent (Life technologies, US) as described (Gao et al. 2016). Library construction and sequencing with an Illumina HiseqTM2000 sequencer were performed at Shanghai Biotechnology Corporation (Shanghai, China). Over 25 Mb high-quality RNA-seq reads (deposited at the NCBI Sequence Read Archive database under the accession code of SRP062439) were obtained for each sample and mapped onto the reference genome of *F. graminearum* with Tophat2 (http://ccb.jhu.edu/software/tophat/index.shtml). The intron retention level was calculated as the percentage of reads with the predicted intron sequence over its transcripts. Weakly expressed genes were filtered out by excluding transcripts with less than 1 count per million reads in the analysis. For each intron, changes in the intron retention level in suppressor S2 were calculated in comparison with PH-1 and FP1 (Gao et al. 2016).

Yeast two-hybrid assays

Protein–protein interactions were assayed with the Matchmaker yeast two-hybrid system (Clontech, Mountain View, CA, USA). Fragments or entire ORF of *FgPRP6, FgPRP31*, and *FgBRR2* were amplified from first-strand cDNA of PH-1 with primers listed in Table S1 and cloned into the pGBKT7 or pGADT7 vector. To generate bait or prey constructs of *FgPRP6, FgPRP31*, and *FgBRR2* carrying various suppressor mutations, first-strand cDNA of corresponding suppressor strains were used for PCR amplification. The resulting bait and prey construct were confirmed by sequencing analysis and transformed in pairs into yeast strain AH109 (Clontech). The Leu^+ Trp^+ transformants were isolated and assayed for growth on SD-Trp-Leu-His medium and galactosidase (LacZ) activities with filter lift assays as described (Zhou et al. 2011b) with the positive and negative controls provided in the Matchmaker library construction kit (Clontech).

Co-IP assays

The *FgPRP31*^{WT}-, *FgPRP31*^{N463}-, *FgPRP31*^{G529D}-, and *FgPRP31*^{D534G}-3×FLAG constructs were generated by transforming fragments of *FgPRP31* amplified from PH-1 or corresponding suppressors together with *Xho*I-digested pFL7 into yeast strain XK1-25 as described (Bourett et al. 2002; Bruno et al. 2004). The FLAG-tag fusion constructs were rescued from the resulting Trp^+ yeast transformants and confirmed by sequencing analysis. The same yeast gap repair approach was used to generate the *FgPRP31*^{CT}- and *FgPRP6*-GFP constructs with vector pFL2 (Zhou et al. 2011a). The resulting GFP- and FLAG-fusion constructs were transformed in pairs into protoplasts of PH-1 as described (Hou et al. 2002). Transformants resistant to both hygromycin and geneticin were isolated and confirmed for the expression of transforming vectors by western blot analysis. For co-IP assays, total proteins isolated from vegetative hyphae (Bruno et al. 2004) were mixed with anti-FLAG or anti-GFP beads (Sigma-Aldrich) and proteins bounds to the beads were eluted as described (Zhou et al. 2011b). Western blots of proteins separated on 10% SDS PAGE gels and transferred to nitrocellulose membranes (Amersham, Piscataway, NJ, USA) were detected with the anti-GFP (Sigma-Aldrich) and anti-FLAG (Sigma-Aldrich) antibodies (Liu et al. 2011).

Phosphorylation assays

For phosphorylation assays, total proteins were isolated from *FgPRP31*-GFP transformants of PH-1 and *Fgprp4* suppressor strain S47 (Table 1) as described (Bruno et al. 2004) and incubated with anti-GFP beads (Sigma). Proteins eluted from anti-GFP beads were separated on 10% SDS PAGE gels and transferred to nitrocellulose membranes. Western blots of proteins eluted from anti-GFP beads was detected with the anti-GFP (Sigma-Aldrich) and anti-phosphoserine (anti-pSer) (Abcam Cambridge, MA, USA) antibodies as described (Xie et al. 2014). Detection with pIMAGO (Tymora Analytical Operations, West Lafayette, IN, USA) was performed as described (Iliuk et al. 2011).

BiFC assays

The *FgPRP31*-YFPN, *FgPRP6*-YFPC, and *FgBRR2*-YFPC fusion constructs were generated by cloning their coding regions amplified from PH-1 into the BiFC vectors pHZ65 and pHZ68 (Zhao and Xu 2007), respectively, by the yeast gap repair approach (Bourett et al. 2002; Bruno et al. 2004). Similar approaches were used to generate the *FgPRP31*^{N463}-YFPN and *FgPRP31*^{L532P}-YFPN constructs. The resulting YFP fusion constructs of different *FgPRP31* alleles were confirmed by sequencing analysis and transformed in pairs into protoplasts of PH-1. Transformants resistant to both hygromycin and geneticin were screened by PCR and examined under a Nikon epifluorescence microscope for YFP signals.

Generation of transformants expressing constitutive negative mutant (S/T-A) alleles of *FgPRP31*

To generate the *FgPRP31*$^{S485A\ S486A}$-GFP construct by yeast gap repair (Chen et al. 2014), the N- and C-terminal fragments of *FgPRP31* were amplified with primer pairs PRP31F/SSAR and SSAF/PRP31R (Table S1), respectively. SSAR and SSAF were overlapping primers to introduce the S485A S486A mutations. These two fragments were co-transformed with *Xho*I-digested vector pDL2 that carries the HygR hygromycin-resistance marker (Zhou et al. 2011a) into yeast strain XK1-25 (Bruno et al. 2004). The resulting fusion construct rescued from Trp^{+} yeast transformants was confirmed by sequencing analysis. The *FgPRP31*$^{S485A\ S486A}$-GFP construct was then co-transformed into PH-1 with the *FgPRP31* gene replacement generated by split-marker with the geneticin-resistance marker amplified from pFL2 (Zhou et al. 2011a). The *FgPRP31*$^{S520A\ S521A\ T525A}$-GFP construct was generated with similar approaches and co-transformed into PH-1 with the *FgPRP31* gene replacement construct. The resulting transformants resistant to both geneticin and hygromycin were screened for *FgPRP31* deletion and examined for the integration of *FgPRP31*$^{S485A\ S486A}$-GFP or *FgPRP31*$^{S520A\ S521A\ T525A}$-GFP constructs by PCR and GFP signals.

Generation of transformants expressing dominant active mutant (S/T-D) alleles of *FgPRP31*

The same yeast gap repair approach (Bruno et al. 2004) was used to generate the *FgPRP31*$^{S485D\ S486D}$-GFP and *FgPRP31*$^{S520D\ S521D\ T525D}$-GFP constructs with *Xho*I-digested plasmid pFL2 carrying the geneticin-resistance marker (Zhou et al. 2011a). Primers used to introduce the S485D S486D or S520D S521D T525D mutations were listed in Table S1. Similar strategies were used to generate the *FgPRP31*^{S520D}-, *FgPRP31*^{S521D}-, and *FgPRP31*^{T525D}-GFP fusion constructs. All the mutant alleles of *FgPRP31* were confirmed by sequencing analysis and co-transformed into protoplasts of PH-1 with the *FgPRP4* knockout construct (Wang et al. 2011). Transformants resistant to both geneticin and hygromycin were screened by PCR for deletion of *FgPRP4* and examined for GFP signals for the expression of *FgPRP31* mutant alleles.

Acknowledgements We thank Drs. Chenfang Wang, Cong Jiang, Huiquan Liu, and Anton Iliuk for fruitful discussions. We also thank Dr. Yimei Zhang and Ms. Xiaoping Li for assistance with the yeast two-hybrid and co-IP assays. This work was supported by Grants from the Nature Science Foundation of China (31600117), US Wheat and Barley Scab Initiative (106616), and Fundamental Research Funds for the Central Universities (2452016019).

Author contributions Conceived and designed the experiments: XG, QJ, JRX. Performed the experiments: XG, CS, JZ, KY, JW. Analyzed the data: XG, QJ, JRX. Contributed reagents/materials/analysis tools: XG, QJ. Wrote the paper: XG, QJ, JRX.

References

Absmeier E, Wollenhaupt J, Mozaffari-Jovin S, Becke C, Lee CT, Preussner M, Heyd F, Urlaub H, Lührmann R, Santos KF, Wahl MC (2015) The large N-terminal region of the Brr2 RNA helicase guides productive spliceosome activation. Genes Dev 29:2576–2587

Agafonov DE, Kastner B, Dybkov O, Hofele RV, Liu WT, Urlaub H, Lührmann R, Stark H (2016) Molecular architecture of the human U4/U6.U5 tri-snRNP. Science 351:1416–1420

Bertram K, Agafonov DE, Dybkov O, Haselbach D, Leelaram MN, Will CL, Urlaub H, Kastner B, Lührmann R, Stark H (2017) Cryo-EM structure of a pre-catalytic human spliceosome primed for activation. Cell 170:701–713 e711. https://doi.org/10.1016/j.cell.2017.07.011

Boesler C, Rigo N, Anokhina MM, Tauchert MJ, Agafonov DE, Kastner B, Urlaub H, Ficner R, Will CL, Lührmann R (2016) A spliceosome intermediate with loosely associated tri-snRNP accumulates in the absence of Prp28 ATPase activity. Nat Commun 7:11997

Bottner CA, Schmidt H, Vogel S, Michele M, Kaufer NF (2005) Multiple genetic and biochemical interactions of Brr2, Prp8, Prp31, Prp1 and Prp4 kinase suggest a function in the control of the activation of spliceosomes in *Schizosaccharomyces pombe*. Curr Genet 48:151–161. https://doi.org/10.1007/s00294-005-0013-6

Bourett TM, Sweigard JA, Czymmek KJ, Carroll A, Howard RJ (2002) Reef coral fluorescent proteins for visualizing fungal pathogens. Fungal Genet Biol 37:211–220

Bruno KS, Tenjo F, Li L, Hamer JE, Xu JR (2004) Cellular localization and role of kinase activity of PMK1 in *Magnaporthe grisea*. Eukaryot Cell 3:1525–1532. https://doi.org/10.1128/EC.3.6.1525-1532.2004

Chen D, Wang Y, Zhou X, Wang Y, Xu JR (2014) The Sch9 kinase regulates conidium size, stress responses, and pathogenesis in *Fusarium graminearum*. PLoS One 9:e105811. https://doi.org/10.1371/journal.pone.0105811

Church M, Smith KC, Alhussain MM, Pennings S, Fleming AB (2017) Sas3 and Ada2(Gcn5)-dependent histone H3 acetylation is required for transcription elongation at the de-repressed FLO1 gene. Nucleic Acids Res 45:4413–4430. https://doi.org/10.1093/nar/gkx028

Cuomo CA, Güldener U, Xu JR et al (2007) The *Fusarium graminearum* genome reveals a link between localized polymorphism and pathogen specialization. Science 317:1400–1402. https://doi.org/10.1126/science.1143708

Fair FJ, Pleiss JA (2017) The power of fission: yeast as a tool for understanding complex splicing. Curr Genet 63:375–380

Figueroa M, Hammond-Kosack KE, Solomon PS (2017) A review of wheat diseases—a field perspective. Mol Plant Pathol. https://doi.org/10.1111/mpp.12618

Galej WP, Oubridge C, Newman AJ, Nagai K (2013) Crystal structure of Prp8 reveals active site cavity of the spliceosome. Nature 493:638–643. https://doi.org/10.1038/nature11843

Gao X, Jin Q, Jiang C, Li Y, Li C, Liu H, Kang Z, Xu JR (2016) FgPrp4 kinase is important for spliceosome B-complex activation

and splicing efficiency in *Fusarium graminearum*. PLoS Genet 12:e1005973. https://doi.org/10.1371/journal.pgen.1005973

Goswami RS, Xu JR, Trail F, Hilburn K, Kistler HC (2006) Genomic analysis of host-pathogen interaction between *Fusarium graminearum* and wheat during early stages of disease development. Microbiology 6:1877–1890

Hendler A, Medina EM, Buchler NE, de Bruin RAM, Aharoni A (2017) The evolution of a G1/S transcriptional network in yeasts. Curr Genet. https://doi.org/10.1007/s00294-017-0726-3

Hou Z, Xue C, Peng Y, Katan T, Kistler HC, Xu JR (2002) A mitogen-activated protein kinase gene (MGV1) in *Fusarium graminearum* is required for female fertility, heterokaryon formation, and plant infection. Mol Plant Microbe Interact 15:1119–1127. https://doi.org/10.1094/MPMI.2002.15.11.1119

Iliuk A, Martinez JS, Hall MC, Tao WA (2011) Phosphorylation assay based on multifunctionalized soluble nanopolymer. Anal Chem 83:2767–2774. https://doi.org/10.1021/ac2000708

Janke C, Ortiz J, Lechner J, Shevchenko A, Shevchenko A, Magiera MM, Schramm C, Schiebel E (2001) The budding yeast proteins Spc24p and Spc25p interact with Ndc80p and Nuf2p at the kinetochore and are important for kinetochore clustering and checkpoint control. EMBO J 20:777–791. https://doi.org/10.1093/emboj/20.4.777

Jiang C, Xu JR, Li HQ (2016) Distinct cell cycle regulation during saprophytic and pathogenic growth in fungal pathogens. Curr Genet 62:185–189

Kazi T, Islam PB, Fakhoury AM (2017) *FvSNF1*, the sucrose non-fermenting protein kinase gene of *Fusarium virguliforme*, is required for cell-wall-degrading enzymes expression and sudden death syndrome development. Curr Genet 63:723–738

Kuhn AN, Kaufer NF (2003) Pre-mRNA splicing in *Schizosaccharomyces pombe*: regulatory role of a kinase conserved from fission yeast to mammals. Curr Genet 42:241–251

Kuhn AN, Reichl EM, Brow DA (2002) Distinct domains of splicing factor Prp8 mediate different aspects of spliceosome activation. Proc Natl Acad Sci USA 99:9145–9149

Li Y, Zhang X, Hu S, Liu H, Xu JR (2017) PKA activity is essential for relieving the suppression of hyphal growth and appressorium formation by MoSfl1 in *Magnaporthe oryzae*. PLoS Genet 13:e1006954. https://doi.org/10.1371/journal.pgen.1006954

Liu S, Rauhut R, Vornlocher HP, Luhrmann R (2006) The network of protein–protein interactions within the human U4/U6.U5 tri-snRNP. RNA 12:1418–1430. https://doi.org/10.1261/rna.55406

Liu S, Li P, Dybkov O, Nottrott S, Hartmuth K, Lührmann R, Carlomagno T, Wahl MC (2007) Binding of the human Prp31 Nop domain to a composite RNA-protein platform in U4 snRNP. Science 316:115–120. https://doi.org/10.1126/science.1137924

Liu W, Zhou X, Li G, Li L, Kong L, Wang C, Zhang H, Xu JR (2011) Multiple plant surface signals are sensed by different mechanisms in the rice blast fungus for appressorium formation. PLoS Pathog 7:e1001261. https://doi.org/10.1371/journal.ppat.1001261

Liu H, Zhang S, Ma J, Dai Y, Li C, Lyu X, Wang C, Xu JR (2015) Two Cdc2 Kinase genes with distinct functions in vegetative and infectious hyphae in *Fusarium graminearum*. PLoS Pathog 11:e1004913. https://doi.org/10.1371/journal.ppat.1004913

Makarova OV, Makarov EM, Liu S, Vornlocher HP, Luhrmann R (2002) Protein 61K, encoded by a gene (PRPF31) linked to autosomal dominant retinitis pigmentosa, is required for U4/U6·U5 tri-snRNP formation and pre-mRNA splicing. EMBO J 21:1148–1157. https://doi.org/10.1093/emboj/21.5.1148

McKay SL, Johnson TL (2010) A bird's-eye view of post-translational modifications in the spliceosome and their roles in spliceosome dynamics. Mol Biosyst 6:2093–2102. https://doi.org/10.1039/c002828b

Mozaffari-Jovin S, Santos KF, Hsiao HH, Will CL, Urlaub H, Wahl MC, Luhrmann R (2012) The Prp8 RNase H-like domain inhibits Brr2-mediated U4/U6 snRNA unwinding by blocking Brr2 loading onto the U4 snRNA. Genes Dev 26:2422–2434. https://doi.org/10.1101/gad.200949.112

Mozaffari-Jovin S, Wandersleben T, Santos KF, Will CL, Luhrmann R, Wahl MC (2013) Inhibition of RNA helicase Brr2 by the C-terminal tail of the spliceosomal protein Prp. 8 Science 341:80–84. https://doi.org/10.1126/science.1237515

Nguyen TH, Galej WP, Bai XC, Savva CG, Newman AJ, Scheres SH, Nagai K (2015) The architecture of the spliceosomal U4/U6.U5 tri-snRNP. Nature 523:47–52. https://doi.org/10.1038/nature14548

Schneider M, Hsiao HH, Will CL, Giet R, Urlaub H, Luhrmann R (2010) Human PRP4 kinase is required for stable tri-snRNP association during spliceosomal B complex formation. Nat Struct Mol Biol 17:216–221. https://doi.org/10.1038/nsmb.1718

Theuser M, Hobartner C, Wahl MC, Santos KF (2016) Substrate-assisted mechanism of RNP disruption by the spliceosomal Brr2 RNA helicase. Proc Natl Acad Sci USA 113:7798–7803. https://doi.org/10.1073/pnas.1524616113

Vithana EN, Abu-Safieh L, Allen MJ et al (2001) A human homolog of yeast pre-mRNA splicing gene, PRP31, underlies autosomal dominant retinitis pigmentosa on chromosome 19q13.4 (RP11). Mol Cell 8:375–381

Wan R, Yan C, Bai R, Huang G, Shi Y (2016a) Structure of a yeast catalytic step I spliceosome at 3.4 A resolution. Science 353:895–904. https://doi.org/10.1126/science.aag2235

Wan R, Yan C, Bai R, Wang L, Huang M, Wong CC, Shi Y (2016b) The 3.8 A structure of the U4/U6.U5 tri-snRNP: insights into spliceosome assembly and catalysis. Science 351:466–475. https://doi.org/10.1126/science.aad6466

Wang C, Zhang S, Hou R et al (2011) Functional analysis of the kinome of the wheat scab fungus *Fusarium graminearum*. PLoS Pathog 7:e1002460

Weidenhammer EM, Singh M, Ruiz-Noriega M, Woolford JL (1996) The PRP31 gene encodes a novel protein required for pre-mRNA splicing in *Saccharomyces cerevisiae*. Nucleic Acids Res 24:1164–1170

Weidenhammer EM, Ruiz-Noriega M, Woolford JL (1997) Prp31p promotes the association of the U4/U6 × U5 tri-snRNP with pre-spliceosomes to form spliceosomes in *Saccharomyces cerevisiae*. Mol Cell Biol 17:3580–3588

Will CL, Luhrmann R (2011) Spliceosome structure and function. Cold Spring Harb Perspect Biol. https://doi.org/10.1101/cshperspect.a003707

Xie F, Sun S, Xu A, Zheng S, Xue M, Wu P, Zeng JH, Bai L (2014) Advanced oxidation protein products induce intestine epithelial cell death through a redox-dependent, c-jun N-terminal kinase and poly (ADP-ribose) polymerase-1-mediated pathway. Cell Death Dis 5:e1006. https://doi.org/10.1038/cddis.2013.542

Yang C, Liu H, Li G, Liu M, Yun Y, Wang C, Ma Z, Xu JR (2015) The MADS-box transcription factor FgMcm1 regulates cell identity and fungal development in *Fusarium graminearum*. Environ Microbiol 17:2762–2776. https://doi.org/10.1111/1462-2920.12747

Zhao X, Xu JR (2007) A highly conserved MAPK-docking site in Mst7 is essential for Pmk1 activation in *Magnaporthe grisea*. Mol Microbiol 63:881–894

Zhou X, Li G, Xu JR (2011a) Efficient approaches for generating GFP fusion and epitope-tagging constructs in filamentous fungi. Methods Mol Biol 722:199–212

Zhou X, Liu W, Wang C, Xu Q, Wang Y, Ding S, Xu JR (2011b) A MADS-box transcription factor MoMcm1 is required for male fertility, microconidium production and virulence in *Magnaporthe oryzae*. Mol Microbiol 80:33–53